Fluorescence lifetime endoscopy using TCSPC for the measurement of FRET in live cells

Gilbert O. Fruhwirth,[1,2] Simon Ameer-Beg,[1,2] Richard Cook,[3] Timothy Watson,[3] Tony Ng,[1,2] and Frederic Festy[3,*]

[1]*King's College London, The Richard Dimbleby Department of Cancer Studies, Division of Cancer, Guy's Medical School Campus, SE1 1UL, London, United Kingdom*
[2]*King's College London, Randall Division of Cellular and Molecular Biophysics, Guy's Medical School Campus, SE1 1UL, London, United Kingdom*
[3]*King's College London, Dental Institute, Biomaterials Biomimetics and Biophotonics Research Group, SE1 9RT, London, United Kingdom*
**frederic.festy@kcl.ac.uk*

Abstract: Development of remote imaging for diagnostic purposes has progressed dramatically since endoscopy began in the 1960's. The recent advent of a clinically licensed intensity-based fluorescence micro-endoscopic instrument has offered the prospect of real-time cellular resolution imaging. However, interrogating protein-protein interactions deep inside living tissue requires precise fluorescence lifetime measurements to derive the Förster resonance energy transfer between two tagged fluorescent markers. We developed a new instrument combining remote fiber endoscopic cellular-resolution imaging with TCSPC-FLIM technology to interrogate and discriminate mixed fluorochrome labeled beads and expressible GFP/TagRFP tags within live cells. Endoscopic-FLIM (e-FLIM) data was validated by comparison with data acquired via conventional FLIM and e-FLIM was found to be accurate for both bright bead and dim live cell samples. The fiber based micro-endoscope allowed remote imaging of 4 µm and 10 µm beads within a thick Matrigel matrix with confident fluorophore discrimination using lifetime information. More importantly, this new technique enabled us to reliably measure protein-protein interactions in live cells embedded in a 3D matrix, as demonstrated by the dimerization of the fluorescent protein-tagged membrane receptor CXCR4. This cell-based application successfully demonstrated the suitability and great potential of this new technique for in vivo pre-clinical biomedical and possibly human clinical applications.

OCIS codes: (170.2520) Fluorescence microscopy; (170.2150) Endoscopic imaging; (170.3650 Lifetime-based sensing.

References and links

1. P. Cotton, and C. Williams, Practical gastrointestinal endoscopy (Blackwell Science, 2003).
2. K. Suhling, P. M. French, and D. Phillips, "Time-resolved fluorescence microscopy," Photochem. Photobiol. Sci. **4**(1), 13–22 (2005).
3. Z. Papagatsia, A. Tappuni, T. F. Watson, and R. J. Cook, "Single wavelength micro-endoscopy in non-surgical vascular lesion diagnosis & characterization," J. Microsc. **230**(2), 203–211 (2008).
4. R. El-Gazzar, M. Macluskey, and G. R. Ogden, "Evidence for a field change effect based on angiogenesis in the oral mucosa? A brief report," Oral Oncol. **41**(1), 25–30 (2005).
5. F. Festy, S. M. Ameer-Beg, T. Ng, and K. Suhling, "Imaging proteins in vivo using fluorescence lifetime microscopy," Mol. Biosyst. **3**(6), 381–391 (2007).
6. G. McConnell, J. M. Girkin, S. M. Ameer-Beg, P. R. Barber, B. Vojnovic, T. Ng, A. Banerjee, T. F. Watson, and R. J. Cook, "Time-correlated single-photon counting fluorescence lifetime confocal imaging of decayed and sound dental structures with a white-light supercontinuum source," J. Microsc. **225**(2), 126–136 (2007).
7. W. Becker, H. Hickl, C. Zander, K. H. Drexhage, M. Sauer, S. Siebert, and J. Wolfrum, "Time-resolved detection and identification of single analyte molecules in microcapillaries by time-correlated single photon counting," Rev. Sci. Instrum. **70**(3), 1835–1841 (1999).

#123193 - $15.00 USD Received 3 Feb 2010; revised 31 Mar 2010; accepted 13 Apr 2010; published 12 May 2010

8. T. W. J. Gadella, Jr., T. M. Jovin, and R. M. Clegg, "Fluorescence lifetime imaging microscopy (FLIM): Spatial resolution of microstructures on the nanosecond time scale," Biophys. Chem. **48**(2), 221–239 (1993).
9. C. Buranachai, D. Kamiyama, A. Chiba, B. D. Williams, and R. M. Clegg, "Rapid frequency-domain FLIM spinning disk confocal microscope: lifetime resolution, image improvement and wavelet analysis," J. Fluoresc. **18**(5), 929–942 (2008).
10. E. A. Jares-Erijman, and T. M. Jovin, "FRET imaging," Nat. Biotechnol. **21**(11), 1387–1395 (2003).
11. T. Förster, "Intermolecular energy migration and fluorescence," Ann. Phys. **2**, 55 (1948).
12. L. Stryer, "Fluorescence energy transfer as a spectroscopic ruler," Annu. Rev. Biochem. **47**(1), 819–846 (1978).
13. T. Ng, A. Squire, G. Hansra, F. Bornancin, C. Prevostel, A. Hanby, W. Harris, D. Barnes, S. Schmidt, H. Mellor, P. I. Bastiaens, and P. J. Parker, "Imaging protein kinase Calpha activation in cells," Science **283**(5410), 2085–2089 (1999).
14. T. Ng, D. Shima, A. Squire, P. I. H. Bastiaens, S. Gschmeissner, M. J. Humphries, and P. J. Parker, "PKCalpha regulates beta1 integrin-dependent cell motility through association and control of integrin traffic," EMBO J. **18**, 3909–3923 (1999).
15. F. S. Wouters, and P. I. Bastiaens, "Fluorescence lifetime imaging of receptor tyrosine kinase activity in cells," Curr. Biol. **9**(19), 1127–1130 (1999).
16. F. S. Wouters, P. J. Verveer, and P. I. Bastiaens, "Imaging biochemistry inside cells," Trends Cell Biol. **11**(5), 203–211 (2001).
17. S. Pelet, M. J. R. Previte, and P. T. So, "Comparing the quantification of Forster resonance energy transfer measurement accuracies based on intensity, spectral, and lifetime imaging," J. Biomed. Opt. **11**(3), 034017 (2006).
18. M. Parsons, J. Monypenny, S. M. Ameer-Beg, T. H. Millard, L. M. Machesky, M. Peter, M. D. Keppler, G. Schiavo, R. Watson, J. Chernoff, D. Zicha, B. Vojnovic, and T. Ng, "Spatially distinct binding of Cdc42 to PAK1 and N-WASP in breast carcinoma cells," Mol. Cell. Biol. **25**(5), 1680–1695 (2005).
19. M. Peter, and S. M. Ameer-Beg, "Imaging molecular interactions by multiphoton FLIM," Biol. Cell **96**(3), 231–236 (2004).
20. M. Peter, S. M. Ameer-Beg, M. K. Y. Hughes, M. D. Keppler, S. Prag, M. Marsh, B. Vojnovic, and T. Ng, "Multiphoton-FLIM quantification of the EGFP-mRFP1 FRET pair for localization of membrane receptor-kinase interactions," Biophys. J. **88**(2), 1224–1237 (2005).
21. A. Schönle, M. Glatz, and S. W. Hell, "Four-dimensional multiphoton microscopy with time-correlated single-photon counting," Appl. Opt. **39**(34), 6306–6311 (2000).
22. R. R. Duncan, A. Bergmann, M. A. Cousin, D. K. Apps, and M. J. Shipston, "Multi-dimensional time-correlated single photon counting (TCSPC) fluorescence lifetime imaging microscopy (FLIM) to detect FRET in cells," J. Microsc. **215**(1), 1–12 (2004).
23. V. Calleja, S. M. Ameer-Beg, B. Vojnovic, R. Woscholski, J. Downward, and B. Larijani, "Monitoring conformational changes of proteins in cells by fluorescence lifetime imaging microscopy," Biochem. J. **372**(1), 33–40 (2003).
24. J. Requejo-Isidro, J. McGinty, I. Munro, D. S. Elson, N. P. Galletly, M. J. Lever, M. A. A. Neil, G. W. Stamp, P. M. French, P. A. Kellett, J. D. Hares, and A. K. Dymoke-Bradshaw, "High-speed wide-field time-gated endoscopic fluorescence-lifetime imaging," Opt. Lett. **29**(19), 2249–2251 (2004).
25. D. Elson, J. Requejo-Isidro, I. Munro, F. Reavell, J. Siegel, K. Suhling, P. Tadrous, R. Benninger, P. Lanigan, J. McGinty, C. Talbot, B. Treanor, S. Webb, A. Sandison, A. Wallace, D. Davis, J. Lever, M. Neil, D. Phillips, G. Stamp, and P. French, "Time-domain fluorescence lifetime imaging applied to biological tissue," Photochem. Photobiol. Sci. **3**(8), 795–801 (2004).
26. I. Munro, J. McGinty, N. Galletly, J. Requejo-Isidro, P. M. P. Lanigan, D. S. Elson, C. Dunsby, M. A. Neil, M. J. Lever, G. W. Stamp, and P. M. French, "Toward the clinical application of time-domain fluorescence lifetime imaging," J. Biomed. Opt. **10**(5), 051403 (2005).
27. S. Kumar, C. Dunsby, P. A. A. De Beule, D. M. Owen, U. Anand, P. M. P. Lanigan, R. K. P. Benninger, D. M. Davis, M. A. Neil, P. Anand, C. Benham, A. Naylor, and P. M. French, "Multifocal multiphoton excitation and time correlated single photon counting detection for 3-D fluorescence lifetime imaging," Opt. Express **15**(20), 12548–12561 (2007).
28. K. Makrogianneli, L. M. Carlin, M. D. Keppler, D. R. Matthews, E. Ofo, A. Coolen, S. M. Ameer-Beg, P. R. Barber, B. Vojnovic, and T. Ng, "Integrating receptor signal inputs that influence small Rho GTPase activation dynamics at the immunological synapse," Mol. Cell. Biol. **29**(11), 2997–3006 (2009).
29. S. Prag, M. Parsons, M. D. Keppler, S. M. Ameer-Beg, P. Barber, J. Hunt, A. J. Beavil, R. Calvert, M. Arpin, B. Vojnovic, and T. Ng, "Activated ezrin promotes cell migration through recruitment of the GEF Dbl to lipid rafts and preferential downstream activation of Cdc42," Mol. Biol. Cell **18**(8), 2935–2948 (2007).
30. P. R. Barber, S. M. Ameer-Beg, J. Gilbey, L. M. Carlin, M. Keppler, T. Ng, and B. Vojnovic, "Multiphoton time-domain fluorescence lifetime imaging microscopy: practical application to protein–protein interactions using global analysis," J. R. Soc. Interface **6**(0), 93–105 (2009).
31. H. Morise, O. Shimomura, F. H. Johnson, and J. Winant, "Intermolecular energy transfer in the bioluminescent system of Aequorea," Biochemistry **13**(12), 2656–2662 (1974).
32. E. M. Merzlyak, J. Goedhart, D. Shcherbo, M. E. Bulina, A. S. Shcheglov, A. F. Fradkov, A. Gaintzeva, K. A. Lukyanov, S. Lukyanov, T. W. Gadella, and D. M. Chudakov, "Bright monomeric red fluorescent protein with an extended fluorescence lifetime," Nat. Methods **4**(7), 555–557 (2007).
33. A. J. Vila-Coro, J. M. Rodríguez-Frade, A. Martín De Ana, M. C. Moreno-Ortíz, C. Martínez-A, and M. Mellado, "The chemokine SDF-1alpha triggers CXCR4 receptor dimerization and activates the JAK/STAT pathway," FASEB J. **13**(13), 1699–1710 (1999).

#123193 - $15.00 USD Received 3 Feb 2010; revised 31 Mar 2010; accepted 13 Apr 2010; published 12 May 2010

34. G. J. Babcock, M. Farzan, and J. Sodroski, "Ligand-independent dimerization of CXCR4, a principal HIV-1 coreceptor," J. Biol. Chem. **278**(5), 3378–3385 (2003).
35. R. Maeda-Mamiya, E. Noiri, H. Isobe, W. Nakanishi, K. Okamoto, K. Doi, T. Sugaya, T. Izumi, T. Homma, and E. Nakamura, "In vivo gene delivery by cationic tetraamino fullerene," Procs. Nat. Acad. Sci. **107**(12), 5339–5344 (2010).
36. C. LoPresti, H. Lomas, M. Massignani, T. Smart, and G. Battaglia, "Polymersomes: nature inspired nanometer sized compartments," J. Mater. Chem. **19**(22), 3576–3590 (2009).
37. H. Lomas, M. Massignani, K. A. Abdullah, I. Canton, C. Lo Presti, S. MacNeil, J. Du, A. Blanazs, J. Madsen, S. P. Armes, A. L. Lewis, and G. Battaglia, "Non-cytotoxic polymer vesicles for rapid and efficient intracellular delivery," Faraday Discuss. **139**, 143–159, discussion 213–228, 419–420 (2008).
38. H. Bar, I. Yacoby, and I. Benhar, "Killing cancer cells by targeted drug-carrying phage nanomedicines," BMC Biotechnol. **8**(1), 37 (2008).
39. T. Y. Lee, C. T. Lin, S. Y. Kuo, D. K. Chang, and H. C. Wu, "Peptide-mediated targeting to tumor blood vessels of lung cancer for drug delivery," Cancer Res. **67**(22), 10958–10965 (2007).
40. C. C. Fjeld, W. T. Birdsong, and R. H. Goodman, "Differential binding of NAD+ and NADH allows the transcriptional corepressor carboxyl-terminal binding protein to serve as a metabolic sensor," Proc. Natl. Acad. Sci. U.S.A. **100**(16), 9202–9207 (2003).
41. A. Cobos-Correa, J. B. Trojanek, S. Diemer, M. A. Mall, and C. Schultz, "Membrane-bound FRET probe visualizes MMP12 activity in pulmonary inflammation," Nat. Chem. Biol. **5**(9), 628–630 (2009).

1. Introduction

One of modern medicine's most rapidly expanding non-serological diagnostic technologies has arisen from the development of macroscopic reflection instruments in the 1960's, allowing wide field imaging and tissue biopsy via "non-invasive" endoscopy [1,2]. However, endoscopic biopsies still present a number of drawbacks such as patient discomfort, wound healing, associated tissue morbidity and the histopathologic laboratory processing and interpretation delays. There is a huge clinical pressure to develop high resolution, in situ opto-diagnostic micro-endoscopic technologies with the potential to provide immediate tissue characterization and diagnostic information. This will allow more extensive tissue sampling with little or no consequential tissue morbidity and in clinical practice more timely implementation of appropriate therapies [3]. The ability to survey field change regions and monitor suspicious, pre-malignant and post-therapeutic fields for characteristic molecular or intracellular changes indicative of malignant disease or recurrence over time without multiple biopsies, would offer huge clinical benefits to diagnosis, accuracy of local tissue assessment and monitoring of life threatening diseases throughout the body [4].

Recent advances in fluorescence lifetime imaging have enabled numerous studies of protein-interaction and physiological monitoring at the microscopic level [5]. This mini-revolution of studies was catalyzed first by the improvement in gated and modulated image intensifier technology in wide-field microscopy and latterly by novel light sources [6] and modern signal processing electronics for time-correlated single-photon counting (TCSPC) [7] or frequency domain routes [8,9]. The emergence of these technologies as sophisticated tools for interrogating protein-protein interactions shows great promise in the quantification of the spatio-temporal dynamics of fundamental processes in the cell. Microscopical techniques coupled with immuno-cytochemical methods allow us to preserve and image the relative localization of multiple signaling molecules in cellular compartments under quiescent or stimulated conditions. Whilst a degree of localization of proteins is conferred using these techniques, the spatial resolution afforded by conventional, far-field microscopy is insufficient to resolve the specific inter-relationship between individual protein complexes occurring on the nanometer scale. Measurement of the near-field localization of protein complexes may be achieved by the detection of Förster resonance energy transfer (FRET) between fluorophore-conjugated proteins [10]. FRET is a non-radiative, dipole-dipole coupling process whereby energy from an excited donor fluorophore is transferred to an acceptor fluorophore in close proximity [11,12]. The dependence of the coupling efficiency varies with the inverse sixth power of the distance between acceptor and donor and is described in terms of the Förster radius (distance at which the efficiency of energy transfer is 50%), typically of the order of 1 – 10 nm. Excitation of the donor sensitizes emission from the acceptor that ordinarily would not occur. Since the process depletes the excited state population of the donor, FRET will both reduce the fluorescence intensity and lifetime. The advantage of using donor FLIM to detect

#123193 - $15.00 USD Received 3 Feb 2010; revised 31 Mar 2010; accepted 13 Apr 2010; published 12 May 2010

FRET is its independence from fluorophore concentration, donor-acceptor stoichiometry and light path length and is therefore well suited to studies in intact cells [13–17]. Combined with confocal or multiphoton microscopy, FLIM/FRET techniques allow us to determine populations of interacting protein species on a point-by-point basis at each resolved voxel in the cell [18–23].

The limitations of both single photon and multi-photon fluorescence lifetime imaging have led to the development of a video-rate time-resolved fluorescence lifetime imaging endoscope [24]. The work of French and associates has focused on the development of this technique for clinical applications for distinguishing tissue auto-fluorescence [25,26]. However, the use of a time-gated image intensifier detector implies that a large quantity of photons is "gated-out". This type of instrument is typically very inefficient in detecting low emission fluorescence, leading to modest lifetime resolution. Furthermore, some *a priori* knowledge of the expected fluorescence lifetimes is needed so that appropriate selection of the imaging gate widths can be made. This technique is therefore disadvantageous for measuring FRET in relatively dim samples such as live cells expressing genetically encoded fluorescence proteins interacting with surrounding acceptor fluorophores. Typically, expressible tag-based live cell experiments necessitate two essential optical requirements: i) very high detection efficiency: the number of photons emitted by donor fluorophores is limited as physiological protein concentrations are generally small, ii) high lifetime resolution: biological responses can often be triggered by small interacting protein population, leading to small FRET efficiency.

For FLIM using FRET as a readout of protein-protein interactions, fluorescence lifetime resolutions of the order of 5% [5] of the donor lifetime are desirable for an accurate calculation of FRET efficiency. Fluorescent proteins have typical fluorescence lifetimes in the region of 2 – 2.5 ns and as a consequence, the ability to accurately measure fluorescence lifetime changes of the order of 100 ps is required. Our approach was to investigate the use of single-photon fluorescence excitation laser-scanning TCSPC endoscopy as a method of acquiring fluorescence lifetime data. The modest scanning speed of the proposed technique can therefore be juxtaposed against the absolute lifetime measurement accuracy and photon detection efficiency that can be achieved versus current wide-field technologies. However, with the advent of multi-beam scanning geometries for laser scanning FLIM, this throughput can readily be extended to improve imaging speed [27].

In this article, we present the development of an endoscopic fluorescence lifetime imaging system combining laser scanning time-correlated single-photon counting techniques with a clinically licensed miniature fiber-based micro-endoscope. Data regarding imaging resolution and lifetime measurements are presented and the system is exemplified with a FRET experiment to map protein-protein interaction in live cells embedded in a 3-dimensional matrix, as a basic model of a diseased organ structure in a patient.

2. Experimental setup

2.1 Description of the system

All imaging was performed using a bespoke microscope system constructed around a TE2000e fluorescence microscope (Nikon, Tokyo, Japan) as described elsewhere [28,29]. In brief, excitation was provided by a picosecond 465 nm laser diode (Becker & Hickl GmbH, Berlin, Germany) and scanned into the image plane using an a-focal scanner through a 20 × objective (Nikon PlanFluor, NA 0.2). Time-resolved detection was provided by a non-descanned detection channel with a fast PMT (Hamamatsu, Japan) placed in the re-projected pupil plane and a TCSPC board (SPC830, Becker and Hickl GmbH, Berlin, Germany). Data were collected using a high-quality 510 ± 10 nm band-pass filter (Semrock, USA) to ensure negligible bleed-through from the red fluorescent proteins present in the FRET experiment. The laser power was adjusted to give average photon counting rates of the order of 10^4 – 10^5 photons s^{-1} (0.0001 – 0.001 photons per excitation event), below the maximum counting rate (10^6 photons s^{-1}) afforded by the TCSPC electronics to avoid pulse pile-up. All FLIM images were acquired by accumulating 117 frames for a total acquisition time of 300 s.

#123193 - $15.00 USD Received 3 Feb 2010; revised 31 Mar 2010; accepted 13 Apr 2010; published 12 May 2010

To allow remote sample endoscopic imaging, a clinically approved MKT Proflex S-650 mini-probe (Mauna Kea Technologies, Paris) fiber bundle designed for a non-lifetime intensity-based imaging system, was positioned in the imaging plane of the same 20 × objective and imaged via the non-descanned port of the microscope. Precise alignment of the common fiber plane with the objective imaging plane was achieved by a home-built fiber holder device to insure maximum coupling efficiency from the objective into the fiber bundle. This 600µm field-of-view fiber bundle (NA = 0.2) is a "contact probe" where both ends were polished to a flat surface and contain no focusing optics. The advantage of such bare-ended fiber is to ensure confocal measurements where individual single mode fibers act as a pin hole, thus reducing greatly the out-of-plane sample fluorescence background present in wide field detection modes. The transmission through the entire fiber bundle was measured to be 18 ± 2% across the whole range of fluorescence excitation and emission wavelengths used in all experiments (470 nm – 650 nm). Individual single-mode fibers imaged in reflection display a core diameter of 2.28 ± 0.48 µm and the average distance between each fiber is 2.80 ± 0.21 µm (centre to centre), leading to an optical resolution of about 5 µm.

Adjustment of the electronic delay between signal (start) and reference (stop) was necessary to take into account of the 2 m fiber bundle which introduced a delay of approximately 10 ns. To model a situation similar to clinical endoscopy, the distal end of the fiber was held with a micro-manipulator and immersed directly into a three-dimensional matrix. In all cases, a pulse repetition rate of 20 MHz enabled the time-domain segmentation between prompt auto-fluorescence generated by the fiber face-plate in the imaging plane and that generated by the sample. This noise rejection scheme proved crucial to measure fluorescence lifetimes with high accuracy (< 100 ps) as the signal-to-noise ratio increased from 2.4 to 6.0 when switching from no noise discrimination to a 10 ns discrimination window.

The instrument response was measured from the hyper-Rayleigh scattering obtained from illuminating a 20 nm colloidal gold particle suspension (Sigma–Aldrich Company Ltd., G-1652) with a highly attenuated excitation laser.). Mono-exponential fitting of each image pixel was obtained by iterative re-convolution using the TRI2 analysis package [30]. To further reduce the background noise, we implemented an algorithm that specifically rejected any signal originating from the area between the individual single-mode fibers and grouped together the pixels corresponding to the same single-mode fibers. Wide-field epi-fluorescence images were obtained by combining fluorescence emission using a FITC cube (excitation filter 465 ± 15nm, dichroic 505 nm, emission filter 535 ± 20 nm; Fig. 1A, top panel) and a Cy3 cube (excitation filter 543 ± 15nm, dichroic 570 nm, emission filter 610 ± 37.5nm) recorded on a CCD camera (ORCA-ER, Hamamatsu, Japan) and corrected for small (maximum 3 pixels) misalignment.

#123193 - $15.00 USD Received 3 Feb 2010; revised 31 Mar 2010; accepted 13 Apr 2010; published 12 May 2010

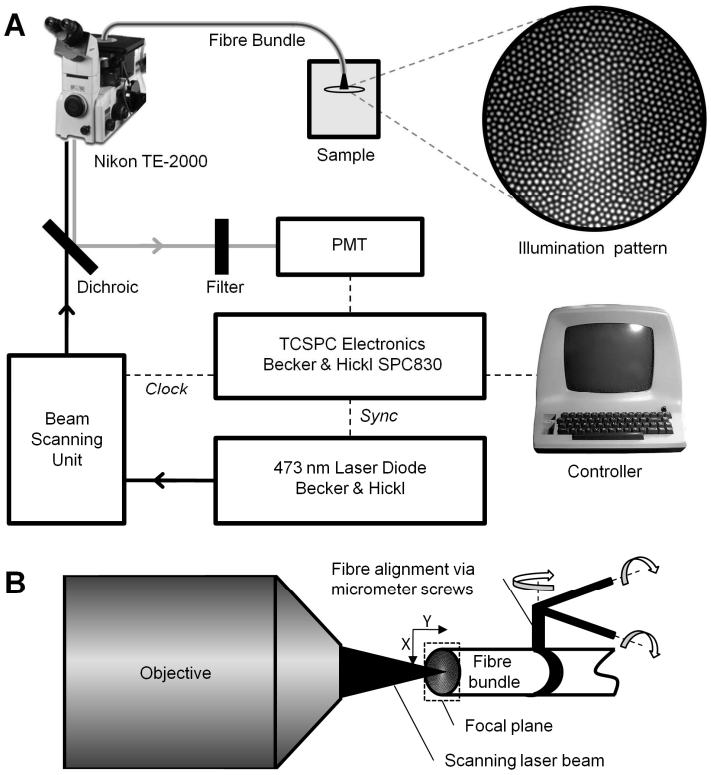

Fig. 1. Schematic drawing of the experimental setup. (A) Main components of the setup are shown including a magnified reflection image of the front of the fiber bundle. The fiber cores have a diameter of 2.28 ± 0.48 µm and are spaced 2.80 ± 0.21 µm apart, leading to an optical resolution of about 5 µm. (B) Illustration of how the fiber bundle is coupled to the objective. The laser beam is scanned over the polished fiber bundle, which is aligned precisely with the focal plane.

2.2 Sample preparation

Preparation of fluorescent microsphere and cell samples within a three-dimensional matrix was performed by suspending known amounts of microspheres or cells in either Matrigel (BD Bioscience, Oxford, UK) or Cygel (Biostatus Ltd., Shepshed, UK) according to the manufacturer's instructions. The gel-bead/cell mix was cast into shapes with 10 × 5 × 5 mm dimensions (length × width × height) to yield jelly-like samples containing beads/cells randomly distributed within its volume. Samples were made freshly for each experiment and were used within six hours of preparation.

In order to perform FRET experiments in living cells, we generated cell lines expressing plasma membrane receptors fused to fluorescent proteins. In brief, the human chemokine receptor CXCR4 was fused to the N-terminus of GFP or TagRFP by sub-cloning its coding sequence between the HindIII and EcoR1 sites of either pEGFP-N1 (Clontech, Saint-Germain-en-Laye, France) or pTagRFP-N1 (Evrogen, Moscow, Russia). The sequences of these C-terminal fusion proteins were then sub-cloned into the retroviral expression vectors pLPCX or pLHCX (Clontech, Saint-Germain-en-Laye, France) and the constructs were confirmed by sequence analysis. Mammary carcinoma cells (MTLn3E) stably expressing human CXCR4-GFP were obtained after retroviral infection, selection with puromycine (1µg/mL), and fluorescence-activated cell sorting (FACS) in order to obtain single clones. A cell line expressing both fluorescent proteins was generated via sequential retroviral infection, selection and FACS-based single clone selection. One single clone of each cell line was

#123193 - $15.00 USD Received 3 Feb 2010; revised 31 Mar 2010; accepted 13 Apr 2010; published 12 May 2010

selected and used for all further experiments. All mammary carcinoma cell lines were cultured in αMEM supplemented with 5% fetal bovine serum, penicillin/streptomycin (100 IU), and *L*-glutamine in an atmosphere containing 5% CO2 (v/v) either in the presence or the absence of the respective selection antibiotic.

Fluorescent microspheres with mean diameters of 10 µm and 4 µm were purchased from Duke Scientific Corporation. All other chemicals used in this study were either from Sigma-Aldrich (Gillingham, UK) or VWR (Lutterworth, UK) unless otherwise specified.

3. Results

The experimental setup described above enabled us to compare fluorescence lifetime images acquired through the fiber bundle (endoscopic mode") or to operate the system as a conventional fluorescence lifetime imaging microscope by removing the fiber bundle ("laboratory microscopic mode"). In initial experiments we used two types of fluorescent microspheres with different fluorescence spectra, brightness and fluorescence lifetimes, immersed them in a gel-based three-dimensional matrix and determined their fluorescence properties in the microscopic mode of the system. The first type of fluorescent microspheres used (10 µm diameter, λ_{max}^{ex} = 468 nm, λ_{max}^{em} = 508 nm) showed green fluorescence if excited through a FITC cube (Fig. 2A, top panel). We then determined the fluorescence lifetime of these microspheres by excitation with a pulsed single-photon laser at 467 nm through a 510 ± 10 nm BP emission filter using TCSPC. The fluorescence lifetime of these beads had a narrow fluorescence lifetime distribution centreed on 2.18 ± 0.09 ns (Fig. 2A, top panel). As a second type, we used smaller microspheres (4 µm diameter, λ_{max}^{ex} = 470 nm, λ_{max}^{em} = 520 nm) which showed broader fluorescence across the green and the orange-red channels (50% of maximum emission at 570 nm) using FITC and Cy3 cubes respectively (Fig. 2A, middle left panel). The color in Fig. 2A appears yellow because of the overlay of green and red fluorescence channels. We determined the fluorescence lifetime of the 4 µm microspheres under the same settings as for the 10 µm microspheres and found the fluorescence lifetime histogram to be much broader with a mean fluorescence lifetime of 4.07 ± 0.43 ns (Fig. 2A, middle panel). The associated fluorescence lifetime images were obtained from the single photon TCSPC data by fitting the photon arrival time histogram with a mono-exponential decay function using the Marquardt algorithm with the resulting histograms plotted next to the fluorescence lifetime maps in Fig. 3. The different fluorescence properties of the two types of microspheres enabled us to distinguish mixtures of them on their excitation/emission characteristics as well as based-on their fluorescence lifetimes (Fig. 2A, bottom panel). While the microsphere sizes might be misleading by not taking into account agglomeration effects, the fluorescence properties clearly allow us to discriminate between them (Fig. 2A, bottom right panel).

Next, we repeated these measurements using the fiber bundle and operated the system as a fluorescence lifetime micro-endoscope. Again, different types of microspheres were immersed either alone or as a mixture in the 3D matrix Cygel and we put the fiber ca. 3 mm into the matrix for imaging. We acquired images by either operating the fiber bundle as a conventional fluorescence endoscope with two channels (FITC and Cy3 fluorescence cubes) or as a fluorescence lifetime endoscope using the pulsed single-photon laser at 467 nm combined with a BP 510 ± 10 nm filter. Imaging the samples through the fiber bundle enabled us to distinguish between the different microsphere types due to their emission characteristics. However, we obtain a decreased image resolution using the fiber bundle, which is due to the diameter and the separation of the individual fibers (compare to section 2.1). While this effect is negligible when imaging the 10 µm microspheres, the resultant pixelation allows for no more than 2 – 3 fibers per particle in the case of the 4 µm microspheres directly positioned on the surface of the fiber (insets of Fig. 2B). As the beads are located a small distance from the bare-end fiber surface, they appeared magnified. Although isolated microspheres are still identifiable, the localization and discrimination between microspheres within aggregates was difficult. However, the fluorescence lifetime distributions of individual microspheres measured through the fiber bundle do not seem to suffer from this resolution constraint. When

#123193 - $15.00 USD Received 3 Feb 2010; revised 31 Mar 2010; accepted 13 Apr 2010; published 12 May 2010

measured through the fiber bundle, the average fluorescence lifetimes of the 10 µm and 4 µm microspheres were determined to be 2.07 ± 0.07 ns and 3.44 ± 0.36 ns, respectively. The fluorescence lifetimes we obtained for the larger microspheres in the endoscopic mode are in excellent agreement with the measurements in the microscopic mode of the system. In the case of the smaller microspheres, we obtained a slightly reduced fluorescence lifetime in the endoscopic mode as compared to the microscopic mode; probably due to higher noise contribution as such small particles are only imaged by a very limited number of fiber cores. Nevertheless, the FWHM of the fluorescence lifetime distributions are comparable to one another in the endoscopic and microscopic modes and both microsphere populations can easily be resolved based on their fluorescence lifetimes (Fig. 2B, bottom panel) using the fiber bundle. The reproducibility of the fluorescence lifetime measurements was good and indicates that TCSPC fluorescence lifetime imaging through a coherent fiber bundle is a reliable technique to record fluorescence lifetime images of small particles embedded within a thick translucent matrix such as Cygel or Matrigel.

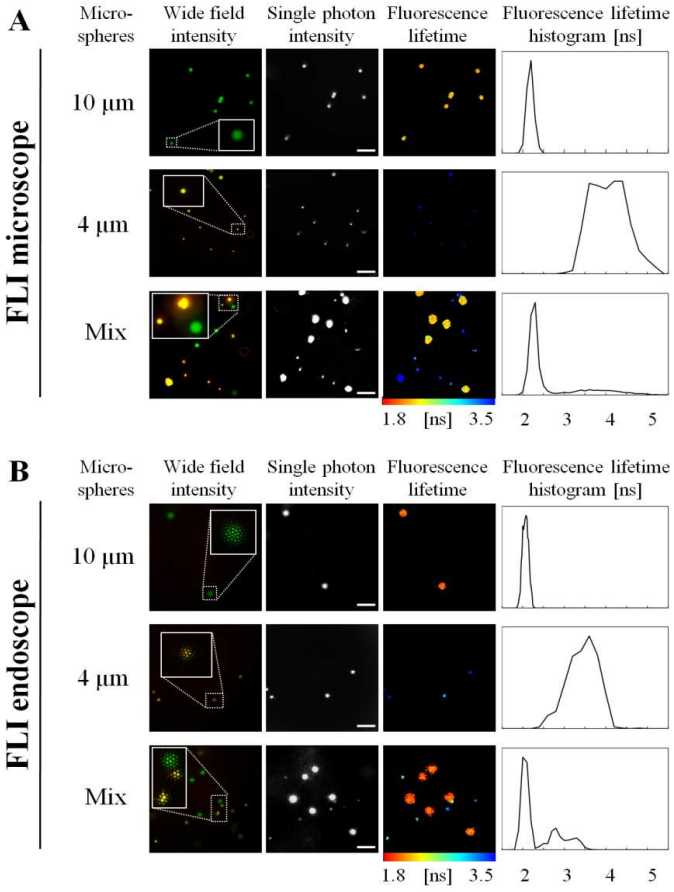

Fig. 2. Comparison of wide-field intensity and single-photon TCSPC FLIM measurements of small beads using either fluorescence lifetime microscopy or endoscopy through a coherent fiber bundle. (A) 10 µm and 4 µm microspheres were immersed alone (top and middle panels, respectively) or as a mixture in a clear 3D matrix and the bottom layer was imaged using a 20-fold objective (0.5 NA, 2.1 mm WD). From the single photon intensity FLIM images the fluorescence lifetime maps were calculated by applying mono-exponential fitting. The right column shows the corresponding fluorescence lifetime histograms. (B) The same samples were used for fluorescence lifetime endoscopy through a coherent fiber bundle of 2 m length and the data are shown as described for (A). Scale bars are 50 µm.

#123193 - $15.00 USD Received 3 Feb 2010; revised 31 Mar 2010; accepted 13 Apr 2010; published 12 May 2010

In order to assess the suitability of this technique in a more biological context, we performed a similar set of experiments with living cells. We generated two cell lines, one expressing a plasma membrane receptor fused to a green fluorescent protein (GFP) [31] and another cell line expressing this fusion protein together with the same receptor, but this time fused to the red fluorescent protein TagRFP (RFP) [32]. We chose the chemokine receptor CXCR4, for these experiments, because it was shown before that this receptor undergoes dimerization at the plasma membrane [33,34]. In the cell line expressing both, CXCR4-GFP and CXCR4-RFP, the receptors co-exist and spontaneously form dimers between the green and the red fluorescent receptor population. This dimer formation brings the two fluorescent proteins in close contact to one another (nm-range) and as a consequence, FRET can occur between two differently tagged receptors (GFP $\rightarrow$ RFP) reducing the fluorescence lifetime of the GFP-tagged receptors. The second cell line expressing solely the green fluorescent CXCR4-GFP serves as a control in order to determine the fluorescence lifetime of GFP in the absence of a FRET acceptor. The FRET efficiency in % is calculated from Eq. (1), in which τ_D is the fluorescence lifetime measured in cells expressing only the GFP-tagged receptor, while τ_{DA} is the fluorescence lifetime of cells expressing both, donor and acceptor fluorophore-tagged constructs.

$$FRETEff = 1 - \frac{\tau_{DA}}{\tau_D} \tag{1}$$

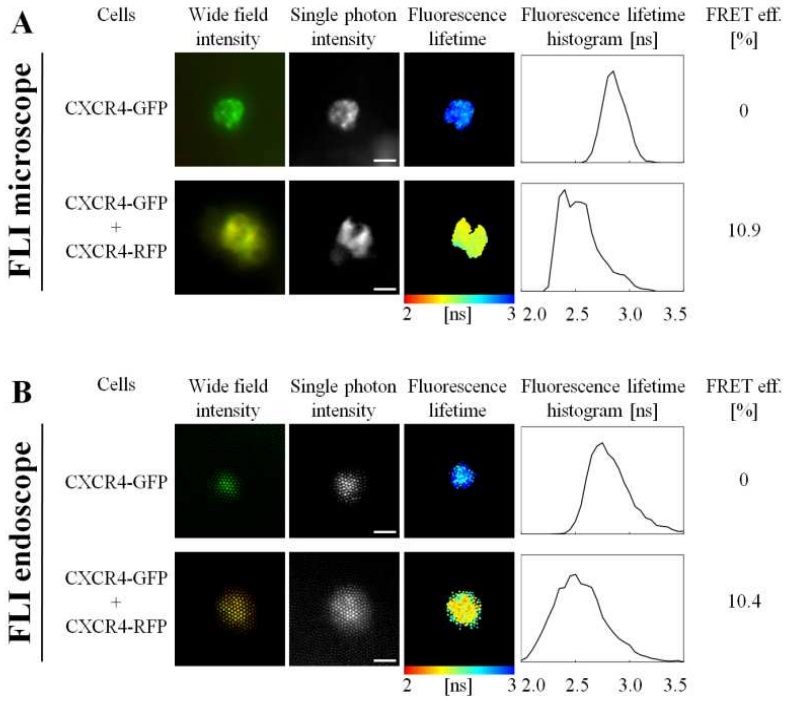

Fig. 3. Fluorescence lifetime endoscopy of living mammalian cells. Wide-field and single-photon TCSPC images of cells expressing CXCR4-GFP and CXCR4-RFP together or CXCR4-GFP alone (control) are shown. The cells expressing both receptors show FRET between GFP and RFP due to receptor dimerization. Fluorescence lifetime maps are calculated from single-photon intensity images and the corresponding histograms are shown next to the fluorescence lifetime maps. (A) Images acquired in the microscopic mode. (B) Images acquired in the endoscopy mode. Scale bars are 20µm.

#123193 - $15.00 USD Received 3 Feb 2010; revised 31 Mar 2010; accepted 13 Apr 2010; published 12 May 2010

All cells were immersed in clear Matrigel for these experiments and were alive during the experiments. When imaging the CXCR4-GFP expressing control cells in the microscopic mode we obtained, as expected, only a signal by using the green filter set in the wide-field mode (Fig. 3A, top panel). Using TCSCP-FLIM, we measured an average fluorescence lifetime of 2.86 ± 0.11 ns (Fig. 3A, N = 5 cells) for the control cell line. With the cell line expressing both constructs, CXCR4-GFP and CXCR4-RFP, we obtained signals in both fluorescence channels in the wide-field mode (Fig. 3A, bottom panel) and measured the average fluorescence lifetime to be 2.55 ± 0.18 ns (Fig. 3A, N = 5 cells). The FRET efficiency between these cells was calculated to be 10.4%. In the endoscopic mode, when imaging through the fiber bundle, we obtained comparable results in the wide-field setup (Fig. 3B, left column). When measuring the fluorescence lifetimes of both cell lines in the endoscopic mode, we obtained an average τ of 2.85 ± 0.24 ns (Fig. 3B, N = 5) for the control cell line and 2.55 ± 0.25 ns (Fig. 3B, N = 11) for the cell line expressing both receptor types. We determined the FRET efficiency between the two cell types to be 10.9%. The pixelation is of negligible importance in the case of live mammalian cells, because of their sizes (~20 μm in this case). The results we obtained through the fiber bundle are in excellent agreement with the measurements in the microscopic mode of our system. Although the presence of the fiber introduces inherent noise from back reflections and reduces the transmission of the sample fluorescence, our results demonstrate that accurate and reproducible FRET measurements by TCSPC-FLIM through such coherent fiber bundle are feasible.

4. Conclusion

The results demonstrated that fluorescence lifetime data can be accurately recorded via miniature fiber endoscopes which are already in clinical use in human medicine and can discriminate dichotomous labeled structures and cells. Similar FRET efficiencies measured in both “endoscopic” and “laboratory microscope” mode indicate that quantitative molecular interaction studies can be carried out in conventionally inaccessible thick samples if suitable labeling strategies can be developed. In vitro and in vivo delivery of fluorophores, contrast agents, reporters, drugs, genes, and nanometer-sized reactors are currently being developed via many routes such as self assembling / disassembling vesicle structures based on phospholipids and fullerenes [35–37], while specific surface binding peptides can increase target tissue affinity and endocytosis for drugs and potential fluorophores by limiting exposure to non-target tissues [38,39]. Tryptophan auto-fluorescence FRET signature changes may be used to report on Nicotinamide adeninine dinucleotide (NAD + / NADH) redox and c-terminal binding protein activity, important in cell differentiation, development, and transformation processes [40]. Soluble FRET reporter molecules, capable of reporting on both extra and intra cellular Matrix Metallo-Proteins (specifically MMP12) have also been used to quantify inflammatory changes in live broncholavage cells in a murine pulmonary inflammation model [41]. The dimensions of the fiber bundles employed in this work are suitable for delivery to remote tissue regions via the same accessory instrument ports, demonstrating the possibilities for technology transfer of the results into in vivo trials. As a consequence, this novel technique not only demonstrates the feasibility of studying complex biological processes such as protein-protein interactions by FRET in cultured living cells within three-dimensional matrices, but, importantly, also provides potential instrumentation to detect other FRET-based assays that may be developed in tissues and organs of whole living organisms.

Acknowledgements

G. Fruhwirth is supported by the King's College London and University College London Comprehensive Cancer Imaging Centre, funded by CR-UK and EPSRC, in association with the MRC and DoH (England) (C1519/A10331). S. Ameer-Beg and T. Ng are supported by an endowment fund from the Dimbleby Cancer Care to King’s College London. Dr. R. Cook was supported by an NIHR Clinician Scientist Fellowship: BS/DHCS/03/G121/55 within King’s College London; T. Watson and F. Festy are supported by the Department of Health via the

#123193 - $15.00 USD Received 3 Feb 2010; revised 31 Mar 2010; accepted 13 Apr 2010; published 12 May 2010

National Institute for Health Research (NIHR) comprehensive Biomedical Research Centre award to Guy's and St. Thomas' NHS Foundation Trust in partnership with King's College London and King's College Hospital NHS Foundation Trust. The fluorescence lifetime system was built with support from both the Medical Research Council Co-Operative Group grant (G0100152 ID 56891) and an UK Research Councils Basic Technology Research Programme grant (GR/R87901/01) and the MKT instruments were funded via a Guy's and St. Thomas Hospitals' Charitable Foundation Diagnostic Technology Development grant and NIHR Clinician Scientist Fellowship: BS/DHCS/03/G121/55 to Dr. Cook. The authors acknowledge financial support from the Department of Health via the National Institute for Health Research (NIHR) comprehensive Biomedical Research Centre award to Guy's and St. Thomas' NHS Foundation Trust in partnership with King's College London.

#123193 - $15.00 USD Received 3 Feb 2010; revised 31 Mar 2010; accepted 13 Apr 2010; published 12 May 2010